Coherent backscattering of Bose-Einstein condensates in two-dimensional disorder potentials

Michael Hartung,[1] Thomas Wellens,[2] Cord A. Müller,[3] Klaus Richter,[1] and Peter Schlagheck[1]

[1]*Institut für Theoretische Physik, Universität Regensburg, 93040 Regensburg, Germany*
[2]*Physikalisches Institut, Albert-Ludwigs Universität Freiburg, 79104 Freiburg, Germany*
[3]*Physikalisches Institut, Universität Bayreuth, 95440 Bayreuth, Germany*

We study quantum transport of an interacting Bose-Einstein condensate in a two-dimensional disorder potential. In the limit of vanishing atom-atom interaction, a sharp cone in the angle-resolved density of the scattered matter wave is observed, arising from constructive interference between amplitudes propagating along reversed scattering paths. Weak interaction transforms this coherent backscattering peak into a pronounced dip, indicating destructive instead of constructive interference. We reproduce this result, obtained from the numerical integration of the Gross-Pitaevskii equation, by a diagrammatic theory of weak localization in presence of a nonlinearity.

PACS numbers: 05.60.Gg; 03.75.Kk; 72.15.Rn

The past years have witnessed an increasing number of theoretical and experimental research activities on the behaviour of ultracold atoms in magnetic or optical disorder potentials [1, 2, 3, 4, 5, 6, 7, 8, 9, 10, 11, 12, 13, 14]. A central aim in this context is the realization and unambiguous identification of strong Anderson localization with Bose-Einstein condensates, which was attempted by several experimental groups [1, 2, 3] with recent success [4, 5], and theoretically studied both from the perspective of the expansion process of the condensate [6] as well as from the scattering perspective [7, 8]. Complementary studies were focused on localization properties of Bogoliubov quasiparticles [9, 10], on dipole oscillations in presence of disorder [11, 12], as well as on the realization of Bose glass phases [13, 14].

The above-mentioned topics mainly refer to processes that are essentially one-dimensional (1D) by nature. Qualitatively new phenomena, however, do arise in two or three spatial dimensions, due to the scenario of *weak localization*. The latter manifests in a slight reduction of the transmission probability of an incident wave through a disordered region as compared to the classically expected value, due to constructive interference between backscattered paths and their time-reversed counterparts. This interference phenomenon particularly leads to a cone-shaped enhancement of the backscattering current in the direction reverse to the incident beam, which was indeed observed [15] and theoretically analyzed [16] in light scattering processes from disordered media. Related weak localization effects also arise in electronic mesoscopic physics, leading to characteristic peaks in the magneto-resistance [17, 18].

In this Letter, we investigate the phenomenon of coherent backscattering with atomic Bose-Einstein condensates that propagate in presence of two-dimensional (2D) disorder potentials. An essential ingredient that comes into play here is the *interaction* between the atoms of the condensate. On the mean-field level, this is accounted for by the nonlinear term in the Gross-Pitaevskii equation describing the time evolution of the condensate wavefunction. Indeed, nonlinearities do also appear in scattering processes of light e.g. from a gas of cold atoms, due to the saturation of the intra-atomic transition [19, 20, 21]. In this case, however, the saturation also leads to inelastic scattering [20, 21] and, in addition, the nonlinearity competes with other dephasing mechanisms induced, e.g., by polarization phenomena [22] or thermal motion [23]. The complementary process of atomic condensates scattering from optical random potentials in the mean-field regime provides a cleaner situation where the coherence of the atomic wavefunction remains well preserved in the presence of the nonlinearity. As we shall argue below, this leads to substantial modifications of the coherent backscattering feature. In particular, the interaction turns constructive into destructive interference, leading to a negative coherent backscattering peak height. This is reminiscent of the weak antilocalization effects due to spin-orbit interaction observed for mesoscopic magneto-transport [24].

The starting point of our investigation is the time-dependent 2D Gross-Pitaevskii equation describing the mean-field dynamics of the condensate in presence of the disorder potential $V(\vec{r})$ [$\vec{r} \equiv (x, y)$],

$$i\hbar\frac{\partial}{\partial t}\psi(\vec{r},t) = \left(-\frac{\hbar^2}{2m}\Delta + V(\vec{r}) + \tilde{g}(x)|\psi(\vec{r},t)|^2\right)\psi(\vec{r},t) + S(t)\delta(x-x_0)\exp(-i\mu t/\hbar)\,, \quad (1)$$

where $S(t)$ denotes a source term simulating the coherent injection of matter waves with chemical potential μ from an external reservoir onto the scattering region [7]. In the numerical integration of Eq. (1), $S(t)$ is adiabatically increased from zero to a final value S_0 that corresponds to a fixed incident current density $j_{\rm in}$. Periodic boundary conditions are imposed on the transverse boundaries (in y direction) of the numerical grid to ensure a homogeneous flow in absence of disorder, whereas absorbing boundary conditions applied at the edges of the longitudinal (x)

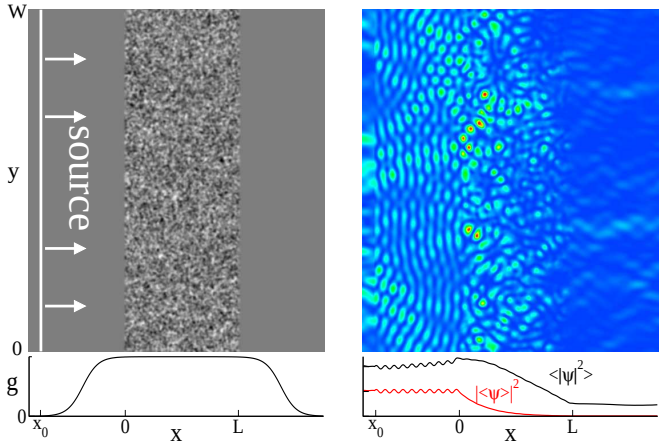

FIG. 1: (Color online) Scattering geometry and stationary scattering state associated with a randomly generated disorder potential. The left-hand side displays $V(x, y)$ in a gray-scale plot and shows the spatial variation of the nonlinearity $g(x)$. The upper right panel shows the density of the corresponding scattering state that is populated through the numerical integration of the inhomogeneous Gross-Pitaevskii equation (1). The lower right panel shows the decay of the coherent mode $|\langle\psi\rangle|^2$ and the density $\langle|\psi|^2\rangle$ with x, averaged over y for $\sim 10^3$ randomly generated disorder configurations. Parameters: $kL = 40$, $kW = 120$, $k\sigma = 0.5$, $V_0 = 0.614\mu$, $g = 0.005$, $j_{\rm in} = \hbar k^3/m$, with $k \equiv \sqrt{2m\mu}/\hbar$.

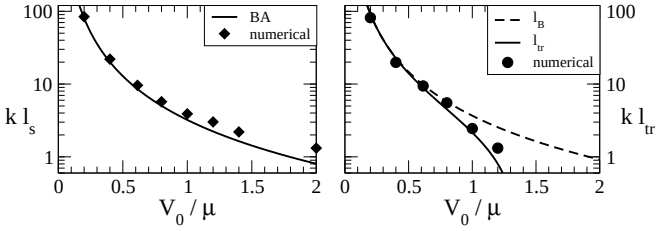

FIG. 2: Scattering mean free path ℓ_s (left panel) and transport mean free path ℓ_{tr} (right panel) in the disorder potential for $k\sigma = 0.5$ in absence of the nonlinearity. In the left panel, the numerically computed lengths are compared with the Born approximation (2) (solid line) and in the right panel with the Boltzmann mean free path (3) (ℓ_B, dashed line) and the expression (4) that takes into account weak localization corrections (ℓ_{tr}, solid line). We find $\ell_{tr} \simeq \ell_s$ for $V_0 < \mu$, which characterizes isotropic scattering.

direction allow us to inhibit artificial backreflection of outgoing waves with rather high accuracy [25].

In Eq. (1), the effective 2D interaction strength is written as $\tilde{g}(x) \equiv \hbar^2 g(x)/(2m)$, with the dimensionless nonlinearity parameter $g(x)$. In presence of a harmonic confinement of the condensate in the third spatial dimension with the oscillator length $a_\perp(x) \equiv \sqrt{\hbar/[m\omega_\perp(x)]}$, we have $g(x) = 4\sqrt{2\pi}a_s/a_\perp(x)$, where a_s denotes the s-wave scattering length of the atoms. We assume that $g(x)$ is adiabatically ramped on and off in front of and behind the disorder region, as shown in Fig. 1. Physically, this spatial variation of the nonlinearity, which is needed in order to avoid nonlinear effects at the position of the source and the absorbing boundaries, would correspond to a finite extent of the transverse harmonic confinement into which the condensate is propagating. As for the disorder potential $V(\vec{r})$, we choose a Gaussian random process characterized by a vanishing mean value $\langle V(\vec{r})\rangle = 0$ and a Gaussian correlation function $\langle V(\vec{r})V(\vec{r}+\Delta\vec{r})\rangle = V_0^2 {\rm e}^{-\Delta r^2/2\sigma^2}$ with correlation length σ. We focus in the following on the parameters $k\sigma = 0.5$, with $k \equiv \sqrt{2m\mu}/\hbar$ the wavenumber of the incident beam, and $V_0/\mu = 0.614$. The incident current density reads $j_{\rm in} = \hbar k|\psi_0|^2/m$, where we set $\psi_0 = k$ for the amplitude of the incident wave [26].

At the above values for σ and V_0, scattering in the disorder region is approximately isotropic. This is quantitatively expressed by the equivalence of the two relevant length scales that the disorder averages introduces for the transport process of the condensate: the scattering mean free path ℓ_s, which describes the average decay of the incident coherent mode inside the disorder region according to $|\langle\psi(\vec{r})\rangle|^2 \propto \exp(-x/\ell_s)$, and the transport mean free path $\ell_{\rm tr}$, which characterizes the decay of the average density $\langle|\psi(\vec{r})|^2\rangle$ (see Fig. 1). In absence of the nonlinearity, the scattering mean free path is in leading order in V_0 given by the Born approximation

$$(k\ell_s)^{-1} \simeq (\pi/2)(V_0/\mu)^2(k\sigma)^2 I_0(k^2\sigma^2)\exp(-k^2\sigma^2) \quad (2)$$

where $I_j(\xi)$ is the modified Bessel function of order j.

The transport mean free path can be extracted from the linear decrease of $\langle|\psi(\vec{r})|^2\rangle$ with x according to $\langle|\psi(\vec{r})|^2\rangle \propto (L + z_0\ell_{tr} - x)$, with $z_0 = 0.82$ in two spatial dimensions, and L the longitudinal extent of the disorder region. In lowest order in V_0, $\ell_{\rm tr}$ is given by the Boltzmann transport mean free path ℓ_B defined through

$$\ell_s/\ell_B = 1 - I_1(k^2\sigma^2)/I_0(k^2\sigma^2)\,. \quad (3)$$

Weak localization effects lead to logarithmic corrections that yield for $k\ell_B \gg 1$ [27, 28]

$$\ell_{tr} \simeq \ell_B[1 - 2(k\ell_B)^{-1}\log(L/\ell_B)]. \quad (4)$$

As shown in Fig. 2, the expressions (2) and (4) are in good agreement with the numerically computed values of ℓ_s and ℓ_{tr} for $V_0 < \mu$. Specifically at $k\sigma = 0.5$ and $V_0/\mu = 0.614$, we find $k\ell_s \simeq 9.61$ and $k\ell_{tr} \simeq 9.75$.

The angle-resolved current in backward direction is numerically computed from the decomposition of the reflected wave $\psi_{\rm ref}(x, y) \equiv \psi(x, y) - \psi_0\exp(ikx)$ at fixed position x close to x_0 [where $g(x)$ is negligibly small] into the transverse eigenmodes $\chi_n(y) \sim \exp(in\pi y/W)$, which support outgoing waves into the directions with the angles $\theta_n \equiv \arcsin[2\pi n/(kW)]$. Figure 3 shows the average angular density $j(\theta)$ of the backscattered current, which is normalized such that $\int_0^{2\pi} j(\theta)d\theta = 2\pi$. In the linear

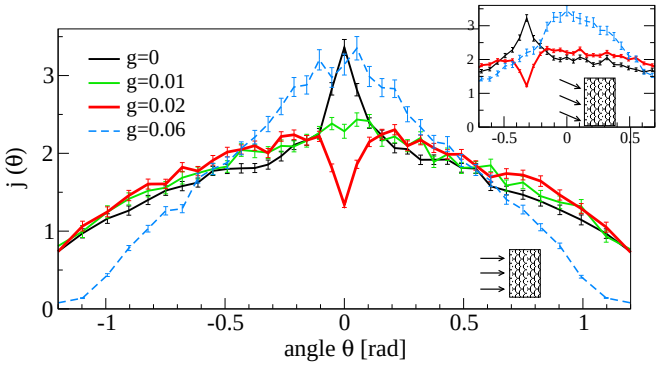

FIG. 3: (Color online) Angle-resolved current density of backscattered atoms in absence and in presence of the nonlinearity, obtained from the average over $\sim 10^3$ disorder configurations (parameters as in Fig. 1; the error bars denote the statistical standard deviation). The coherent backscattering cone for $g = 0$ (black line) is transformed into a pronounced dip for intermediate nonlinearities ($g = 0.02$, bold red line), and turns into a smooth peak structure at larger values of g ($g = 0.06$, dashed blue line). The inset shows the angle-resolved current for the case of a *tilted* incident beam where the source term in Eq. (1) populates the transverse eigenmode defined by the angle $\theta_6 \simeq 0.32$. In contrast to the smooth peak, the cone and dip structures are indeed found at the angle that corresponds to retro-reflection of the incident beam, which confirms that they both arise due to interference between reflected paths.

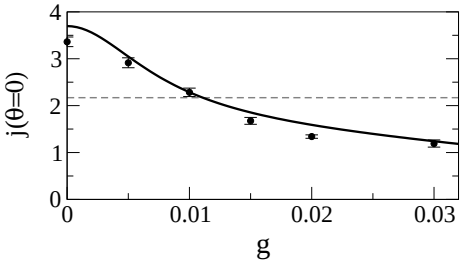

FIG. 4: Backscattered current at $\theta = 0$ as a function of the nonlinearity g (parameters as in Fig. 1), obtained from the numerical simulation (symbols) and from the diagrammatic theory, Eqs. (5-7) (solid line). The horizontal dashed line indicates the diffuse background intensity $j_{\rm L}(0)$. Negative cone heights $j_{\rm C}(0) < 0$ leading to a dip in the angle-resolved current density $j(\theta)$ appear for $g > 0.01$.

case ($g = 0$), we encounter the well-known cone structure at $\theta = 0$, which is a characteristic signature of weak localization [15, 16]. Rather small values of $g \sim 0.02$ corresponding to $\tilde{g}|\psi(\vec{r})|^2 \sim 10^{-2}\mu$, are sufficient to substantially modify this cone-shaped peak. Most interestingly, it is not washed out by the nonlinearity, but transformed into a *dip* that roughly has the same shape as the peak at $g = 0$. This indicates that the underlying interference phenomenon between reflected scattering paths is still effective at finite g, but has turned from constructive to destructive.

The occurence of a dip in the backscattered current is confirmed by calculations based on the diagrammatic approach for weak localization in presence of a nonlinearity [21, 30]. Assuming the realization of a stationary scattering state, the average density $\langle|\psi(\vec{r})|^2\rangle$ is expressed in terms of ladder diagrams, which amounts to neglecting interference, and thus describing wave transport as a classical random walk. This assumption is valid approximately for a dilute medium, i.e. for $k\ell \gg 1$ with $\ell \equiv \ell_B \simeq \ell_{tr} \simeq \ell_s$ (for isotropic scattering). Furthermore, we assume the condition $g^2|\psi_0/k|^4 k\ell \ll 1$ under which scattering from the fluctuations $\tilde{g}|\psi(\vec{r})|^2$ of the nonlinear refractive index is negligible compared to scattering from the disorder potential $V(\vec{r})$ [29]. Therefore, the average density $\langle|\psi(\vec{r})|^2\rangle$ remains approximately unaffected by the nonlinearity, and thus is well described by linear transport theory. From the average density, the flux backscattered in direction $\theta = 0$ results as $j_{\rm L}(0) = \int_0^L dx \exp(-x/\ell)\langle|\psi(x)|^2\rangle/(\ell|\psi_0|^2)$.

In a second step, the coherent backscattering peak is calculated by means of crossed (Cooperon) diagrams, describing interference between reversed scattering paths. Following the diagrammatic approach presented in Ref. [30], we obtain the height of the coherent backscattering peak from the transport equations

$$C_c(x) = |\psi_0|^2 e^{-\hat{x}/\ell}\left(1 + \frac{i}{k}\int_{x_0}^{x} dx' g(x') C_1(x')\right), \quad (5)$$

$$C_1(x) = \int_0^L \frac{dx'}{\pi\ell}\left[K_0\left(\left|\frac{\hat{x}-x'}{\ell}\right|\right)\Big(C_1(x') + C_c(x')\Big) + \right.$$
$$+\frac{i}{k}K_1\left(\left|\frac{\hat{x}-x'}{\ell}\right|\right)\langle|\psi(x')|^2\rangle \times \quad (6)$$
$$\left.\times \int_{\min(x,x')}^{\max(x,x')} dx'' g(x'')\Big(C_1(x'') + C_c(x'')\Big)\right]$$

for the "Cooperon intensity" $C_1(x)$ and the "coherent Cooperon intensity" $C_c(x)$, with $\hat{x} \equiv \max(x, 0)$ and $K_{0,1}$ the modified Bessel functions of the second kind. The contribution to the flux scattered in backward direction then results as

$$j_{\rm C}(0) = {\rm Re}\int_0^L \frac{dx}{\ell|\psi_0|^2} e^{-x/\ell}\Big(C_1(x) + $$
$$+\frac{i}{k}\langle|\psi(x)|^2\rangle\int_{x_0}^{x} dx' g(x') C_1(x')\Big). \quad (7)$$

Note that nonlinear processes also occur for $x_0 < x < 0$ where $V(\mathbf{r}) = 0$ but $g(x) > 0$ (see Fig. 1). Hence, the cone height $j_{\rm C}(0)$ — in contrast to the background intensity $j_{\rm L}(0)$ — explicitly depends on the spatial extent of the nonlinearity region in front of the disorder potential, and can therefore be tuned through the ramp-up of $g(x)$.

In the absence of nonlinearity, the above equations reduce to linear transport theory in a two-dimensional slab, yielding $C_1(x)|_{g=0} = \langle|\psi(x)|^2\rangle - |\psi_0|^2\exp(-x/\ell)$. We

then obtain $j_C(0)|_{g=0} = j_L(0) - 1/2$, which expresses reciprocity symmetry, i.e. the equality of reversed path amplitudes (the term 1/2 describes single scattering). For $g \neq 0$, however, the nonlinearity turns $C_1(x)$ into a complex quantity, as evident from the terms proportional to ig in Eqs. (5-7). This indicates an effective *phase difference* between the reversed scattering paths. Consequently, the backscattered current $j_C(0)$ is expected to decrease with increasing nonlinearity, and may even become negative if this phase difference is sufficiently large.

This latter situation is indeed encountered if the set of equations (5-7) is numerically solved for the system parameters under consideration. As shown in Fig. 4, the total flux $j_L(0) + j_C(0)$ resulting from Eqs. (5-7) (solid line) agrees rather well with the average value for $j(0)$ obtained from the numerical simulation (symbols). Discrepancies are attributed to weak localization corrections in the *background* intensity, which would specifically lead to a reduction of the backscattered flux at $g = 0$, and to an additional contribution to the Cooperon intensity, termed $C_2(x)$ in Ref. [30], which was neglected in the derivation of the above transport equations. Details on these additional ingredients will be presented elsewhere.

At larger nonlinearities, $g \gtrsim 0.03$, the numerical propagation of the inhomogeneous Gross-Pitaevskii equation (1) does not converge to a stationary scattering state, but leads to a permanently time-dependent behaviour of $\psi(\vec{r}, t)$, as predicted in Refs. [29] and encountered also in the transport of condensates through 1D disorder potentials [7]. In this regime, the average backscattered current again displays a peak around $\theta = 0$; this peak is, however, comparatively broad and does not arise from a coherent backscattering phenomenon. This becomes obvious if we inject the incident wave with a *finite angle* $\theta_6 \simeq 0.32$ (corresponding to the transverse eigenmode χ_6) onto the disorder region. While the cone and dip structures at $g = 0$ and 0.02 appear, as shown in the inset of Fig. 3, at the expected angle of coherent backscattering, corresponding to retro-reflection of the incident beam, the broad peak at $g = 0.06$ is not affected in this way.

In conclusion, the presence of a small nonlinearity reverts the scenario of weak localization and gives rise to a cone-shaped dip, instead of a peak, in the angle-resolved backscattered current density. This phenomenon appears to be rather robust; it is numerically encountered also for disorder potentials with longer correlation lengths σ giving rise to anisotropic scattering, and we expect its manifestation also in three spatial dimensions (as predicted by the diagrammatic theory) as well as for speckle disorder where diagrammatic approaches would have to be based on the treatment of Ref. [28]. We therefore believe that the effect would be measurable, for a reasonably large range of parameters, in state-of-the-art transport experiments with coherent Bose-Einstein condensates in well-controlled disorder potentials.

We thank A. Buchleitner, D. Delande, B. Grémaud, R. Kuhn and T. Paul for inspiring discussions. Funding through DFG (Forschergruppe 760) and Bayerisches Eliteförderungsgesetz is gratefully acknowledged.

[1] D. Clément *et al.*, Phys. Rev. Lett. **95**, 170409 (2005).
[2] C. Fort *et al.*, Phys. Rev. Lett. **95**, 170410 (2005).
[3] T. Schulte *et al.*, Phys. Rev. Lett. **95**, 170411 (2005).
[4] J. Billy *et al.*, arXiv:0804.1621 (2008).
[5] G. Roati *et al.*, arXiv:0804.2609 (2008).
[6] L. Sanchez-Palencia *et al.*, Phys. Rev. Lett. **98**, 210401 (2007).
[7] T. Paul, P. Leboeuf, N. Pavloff, K. Richter, and P. Schlagheck, Phys. Rev. A **72**, 063621 (2005).
[8] T. Paul, P. Schlagheck, P. Leboeuf, and N. Pavloff, Phys. Rev. Lett. **98**, 210602 (2007).
[9] N. Bilas and N. Pavloff, Eur. Phys. J. D **40**, 387 (2006).
[10] P. Lugan *et al.*, Phys. Rev. Lett. **98**, 170403 (2007).
[11] J. E. Lye *et al.*, Phys. Rev. A **75**, 061603(R) (2007).
[12] Y. P. Chen *et al.*, Phys. Rev. A **77**, 033632 (2008).
[13] B. Damski, J. Zakrzewski, L. Santos, P. Zoller, and M. Lewenstein, Phys. Rev. Lett. **91**, 080403 (2003).
[14] L. Fallani, J. E. Lye, V. Guarrera, C. Fort, and M. Inguscio, Phys. Rev. Lett. **98**, 130404 (2007).
[15] M. P. Van Albada and A. Lagendijk, Phys. Rev. Lett. **55**, 2692 (1985); P.-E. Wolf and G. Maret, Phys. Rev. Lett. **55**, 2696 (1985).
[16] E. Akkermans, P. E. Wolf, and R. Maynard, Phys. Rev. Lett. **56**, 1471 (1986).
[17] B. L. Altshuler, D. Khmel'nitzkii, A. I. Larkin, and P. A. Lee, Phys. Rev. B **22**, 5142 (1980).
[18] G. Bergmann, Phys. Rep. **107**, 1 (1984).
[19] T. Chanelière, D. Wilkowski, Y. Bidel, R. Kaiser, and C. Miniatura, Phys. Rev. E **70**, 036602 (2004).
[20] V. Shatokhin, C. A. Müller, and A. Buchleitner, Phys. Rev. Lett. **94**, 043603 (2005).
[21] T. Wellens, B. Grémaud, D. Delande, and C. Miniatura, Phys. Rev. A **73**, 013802 (2006).
[22] T. Jonckheere, C. A. Müller, R. Kaiser, C. Miniatura, and D. Delande, Phys. Rev. Lett. **85**, 4269 (2000).
[23] G. Labeyrie, D. Delande, R. Kaiser, and C. Miniatura, Phys. Rev. Lett. **97**, 013004 (2006).
[24] D. M. Zumbühl, J. B. Miller, C. M. Marcus, K. Campman, and A. C. Gossard, Phys. Rev. Lett. **89**, 276803 (2002).
[25] T. Shibata, Phys. Rev. B **43**, 6760 (1991).
[26] A different choice of ψ_0 would amount to rescaling g.
[27] L. P. Gor'kov, A. I. Larkin, and D. E. Khmel'nitskiĭ, Pis'ma Zh. Eksp. Teor. Fiz. **30**, 248 (1979) [JETP Lett. 30, 228 (1979)].
[28] R. C. Kuhn, C. Miniatura, D. Delande, O. Sigwarth, and C. A. Müller, Phys. Rev. Lett. **95**, 250403 (2005); R. C. Kuhn, O. Sigwarth, C. Miniatura, D. Delande, and C. A. Müller, New J. Phys. **9**, 161 (2007).
[29] B. Spivak and A. Zyuzin, Phys. Rev. Lett. **84**, 1970 (2000); J. Opt. Soc. Am B **21**, 177 (2003); S. E. Skipetrov and R. Maynard, Phys. Rev. Lett. **85**, 736 (2000).
[30] T. Wellens and B. Grémaud, Phys. Rev. Lett. **100**, 033902 (2008).